Compositional and structural control in bone regenerative coatings

D. B. HADDOW, M. S. THOMPSON, S. R. BERRY, J. T. CZERNUSZKA
Department of Materials, University of Oxford, Parks Road, Oxford OX1 3PH, UK

The development of a low-temperature method of producing bioactive coatings for medical implants has been shown to bypass the problems associated with high temperature processing routes, in particular the appearance of amorphous phases and non-stoichiometric hydroxyapatite (HA), and delamination of the coating from the substrate. An electric field/aqueous solution technique for producing adherent, crack-free calcium phosphate coatings on titanium and stainless steel substrates is described. The characteristics of the coating are a function of electrode spacing, supersaturation, temperature and current and voltage conditions. Scanning electron microscopy (SEM) characterized the surface morphology of the coatings, which were shown to be HA. The possibility of producing a coating of carbonate-substituted HA having the same chemical composition as bone apatite, and forming at physiological temperatures, has also been demonstrated. The size of the microstructure decreased and the morphology changed as the carbonate ion concentration in the calcium and phosphate ion solution increased.

1. Introduction

Porous monolithic ceramics based on hydroxyapatite (HA) have been shown to aid in osteoconduction of bone when implanted into a bony defect. However, they are too brittle to use in structural applications. One way to overcome this problem is to coat a metallic implant with HA [1–4]. The HA provides the bone bonding capacity while the metal provides the structural support. Unfortunately, all the common forms of producing a coating require elevated temperatures which result in degradation of HA to various calcium phosphate phases depending on the stoichiometry of the starting powder and the cooling rate on coating formation [5].

In order to utilize a wider range of substrates than the metals traditionally used, it is desirable to employ a coating method that does not require elevated processing temperatures. This would open up the possibility of using materials that are traditionally considered bioinert, but may have the necessary strength and toughness to act as implant materials. Several such methods exist, including the biomimetic process [6] and electrophoretic deposition [7]. However, both these methods are substrate specific, and in the case of the biomimetic process the time period for apatite growth is a significant factor. The electric field/aqueous solution method [8] attempts to solve these problems, and has been shown to be applicable to both metallic and coated polymeric materials [9]. An electric field is applied between two electrodes in a solution containing Ca^{2+} and PO_4^{3-} ions. The ions combine to produce calcium phosphate which is then deposited onto the cathode as crystalline HA. The main advantages of this method are that it is a quick, low-temperature process which avoids the problem of producing HA as starting material because the calcium phosphate is formed *in situ*. Incorporation of carbonate ions into the solution allows the formation of a range of coating compositions including HA, carbonate substituted HA and calcium carbonate.

In this study, coatings were characterized by scanning electron microscopy (SEM) and X-ray diffraction (XRD) whilst the solution characteristics for optimum coating production of both stoichiometric HA and carbonate-substituted HA, having the same composition as bone apatite, were determined from the solution supersaturations.

2. Materials and methods

Solutions of 50 mM [Ca] were made up of Ca/P ratio = 5/3 using analytical grade calcium nitrate tetrahydrate, $Ca(NO_3)_2.4H_2O$ and dipotassium hydrogen orthophosphate trihydrate, $K_2HPO_4.3H_2O$ (both Aldrich, UK) in distilled water. Carbonate ions were incorporated using potassium hydrogen carbonate, $KHCO_3$ (Aldrich). Carbonate ions were added to correspond to the following concentrations: (i) carbonate free; (ii) atmospheric CO_2 (1.445×10^{-7} M); (iii) physiological $[CO_3^{2-}]$ (1.6×10^{-6} M); (iv) $[CO_3^{2-}] = 1.5 \times 10^{-4}$ M; and (v) pure carbonate. In the latter case $K_2HPO_4.3H_2O$ was omitted from the stock solution. Into these supersaturated solutions were placed a platinum anode and either a 304 stainless steel or Ti6A14V cathode. The electrodes were connected to a Phillips PM2831 programmable power supply capable of both constant current (CC) and constant voltage (CV) characteristics. Calcium ion concentration, pH and

temperature were monitored using an ION85 meter (Radiometer Ltd, Copenhagen), from which the supersaturation was measured. All experiments were performed at 50 ℃, starting pH 7.4, working solution 1.75 mM [Ca^{2+}], 0.1 M KCl, with a working electrode spacing of 2.25 cm and 2.2 V applied potential. After drying at 60 ℃, gold-coated specimens were examined for surface morphology using a high resolution JEOL 6300 SEM, and phase determination was carried out on a Phillips PW 1710 X-ray diffractometer. Fourier transform infrared (FT-IR) spectroscopy was performed on an ATI Mattson Genesis Series Spectrometer in the wavenumber range 4000–400 cm^{-1}.

3. Results and discussion

3.1. SEM

XRD of coatings deposited in a carbonate free environment indicated that HA was the only phase present (Fig. 1). SEM showed a cellular coating with wall thickness 0.05 μm and a cell size of 0.5 μm (Fig. 2). In addition globules of dimension 5 μm were observed both on top of and in the cell layer (Fig. 3). These spherical globules are amorphous calcium phosphate (ACP) phase, which has previously been postulated to be a precursor to HA [9]. HA nucleates and coalesces into gel sheets within which HA itself is nucleated.

At atmospheric equilibrium [CO_3^{2-}], HA is again the only phase observed. SEM of these coatings showed a secondary, globular phase embedded in the cellular structure (Fig. 4). In this case the cell size had decreased to 0.3 μm and the globules were $\sim$ 2 μm in diameter. At physiological carbonate ion concentration, the cell size decreased to 0.2 μm and correspondingly the globule sizes lay in the range 1–2 μm. HA was the phase produced, and SEM highlighted that as well as the smaller scale of the cellular, honeycomb microstructure, the plates making up the cell walls became more rounded (Fig. 5). At higher carbonate ion concentrations, phases other than HA were observed and these exhibited a flake-like morphology of size 10 μm (Fig. 6). Faint XRD peaks diagnostic of aragonite and calcite suggest that carbonate phases are present. In Fig. 7 a low-voltage SEM micrograph shows the difference in color between carbonated HA and calcium carbonate, which contrasts the image seen in Fig. 6. Although the reason for this change in appearance with accelerating voltage is as yet unresolved, it may prove a useful diagnostic tool for differentiating carbonated HA and carbonate phases within the coatings. For coatings prepared from a solution containing only carbonate and calcium ions, SEM shows a less continuous coating on the electrode, comprising discrete crystallites which have not formed a cellular network. The phase morphology is typified by wheat-grain shaped crystallites which occasionally form

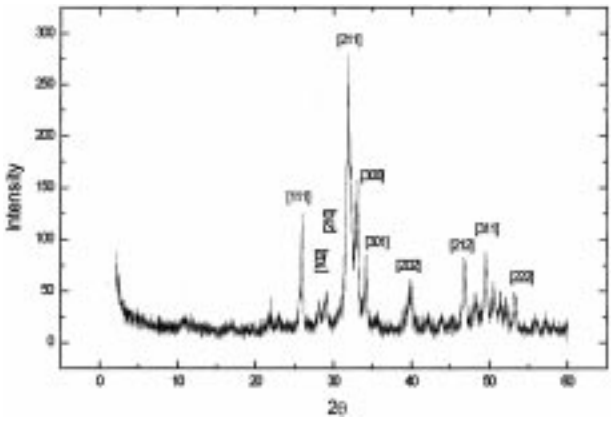

Figure 1 XRD trace of coating prepared at atmospheric carbonate concentration, showing peaks diagnostic of HA.

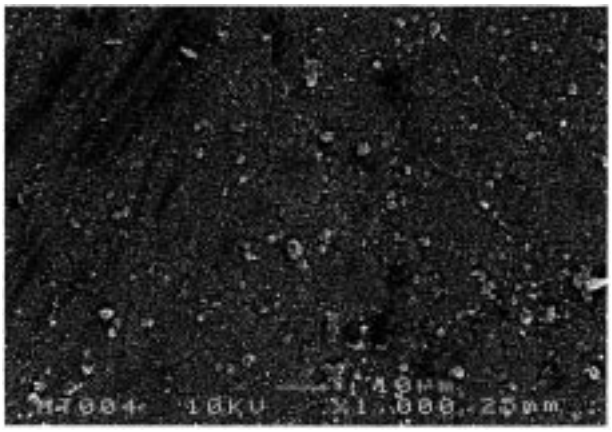

Figure 3 SEM micrograph showing globules embedded in cellular HA.

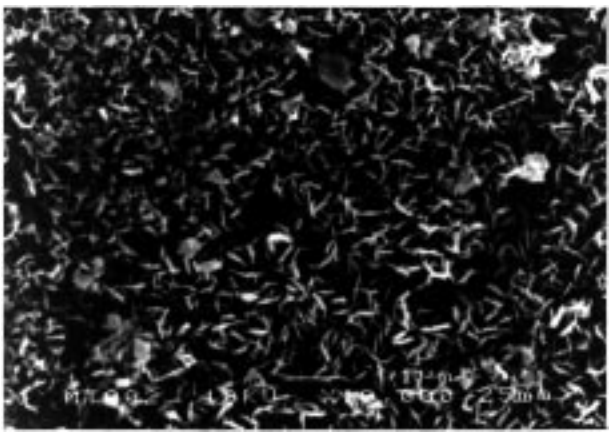

Figure 2 SEM micrograph of HA coating deposited in a carbonate-free environment.

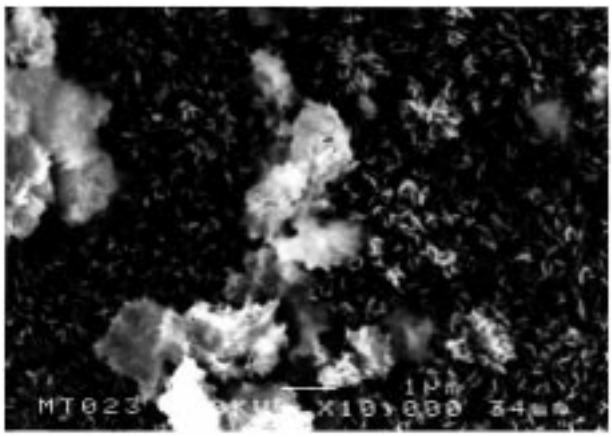

Figure 4 SEM micrograph of HA coating formed with [CO_3^{2-}] = atmospheric HA.

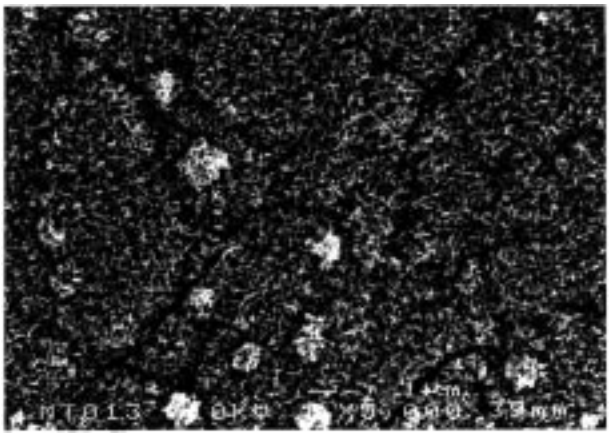

Figure 5 SEM micrograph of coating formed at physiological $[CO_3^{2-}]$.

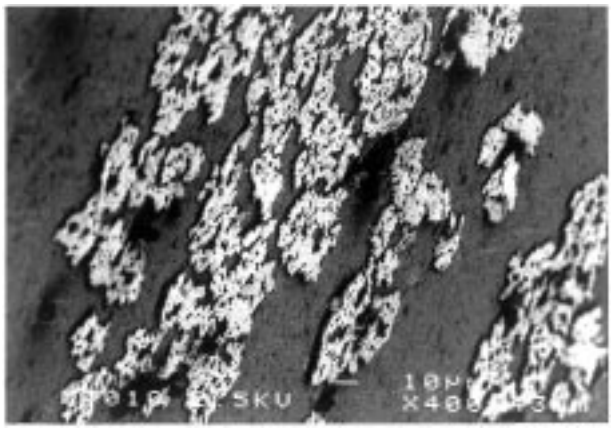

Figure 7 Low voltage SEM of coating formed at $[CO_3^{2-}] = 1.05 \times 10^{-4}$ M, showing changes in coating coloration.

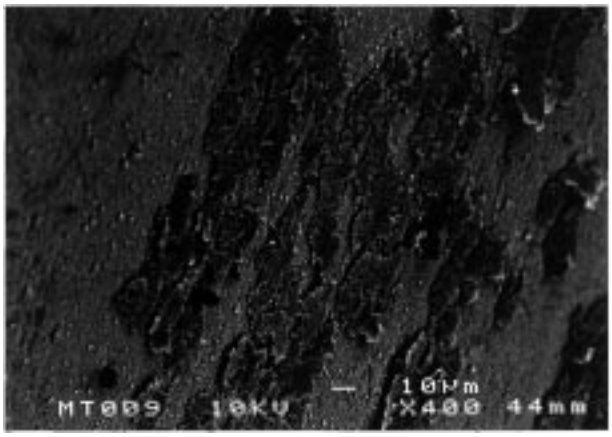

Figure 6 SEM micrograph of coating formed at $[CO_3^{2-}] = 1.05 \times 10^{-4}$ M.

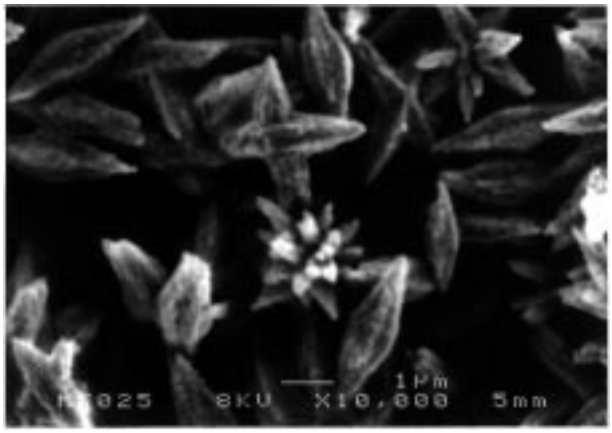

Figure 8 SEM micrograph of pure carbonate coating.

more complex polyhedra (Fig. 8). While the XRD data for the precipitate formed during coating formation exhibit peaks attributable to calcite and aragonite, the SEM micrographs indicate only one phase is present. It was observed that both the cathode and anode were coated during the calcium carbonate deposition process. Given that two phases are detectable by XRD but only one phase is apparent from SEM imaging implies that either (i) both phases appear with the same morphology, or (ii) that one phase has precipitated over a precursor phase, or (iii) phase separation occurred with the aragonite being deposited on the cathode say, and the calcite on the anode. Further work on these aspects is currently in progress to attempt to elucidate which process(es) is/are dominant. The wheat-grain shape exhibits twofold symmetry and is thus more likely to be the orthorhombic aragonite phase. It follows that the precipitate formed on top is the calcite phase. The presence of discrete crystallites on the electrode surface shows that the mechanism of deposition is different to that seen for HA coatings. HA coatings show a gel sheet model of deposition [9], whereby an amorphous phase nucleates, migrates and is deposited, conforming to the substrate surface and coalescing with neighboring sheets to form a coherent covering. Coating integrity therefore appears dependent on the formation of a phase which can act in a similar manner to that of ACP in the calcium phosphate system.

3.2. Supersaturation curves

Supersaturation plots, derived from pH and ion concentration measurements, provide qualitative information about the relative supersaturations of the phosphate and carbonate phases (Fig. 9). When carbonate ions are excluded from the solution HA is always the most supersaturated phase whilst dicalcium phosphate dihydrate (DCPD) remains undersaturated. HA is therefore expected to form in preference to any other phosphate phase. HA precipitation involves a decrease in the number of hydroxyl ions in solution, and therefore a decrease in pH. In contrast, when phosphate ions are completely replaced by carbonate ions, phase deposition is accompanied by a rise in pH. This would indicate that either ACP or carbonate phases should be deposited. Formation of ACP could raise the pH by incorporation of H^+ ions [9], and this mechanism could explain the observed plateau or slight rise in supersaturation of HA when ACP was deposited, because, as proposed earlier, ACP is a precursor to HA formation. ACP has a range of supersaturations, attributable to its variable composition. This has the effect that a range of

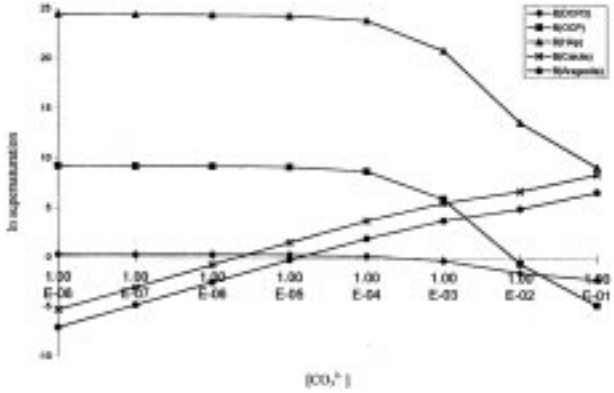

Figure 9 Plot of supersaturation against carbonate ion concentration for CaP and carbonate phases.

carbonate ion concentrations will affect the morphology of the deposited phase rather than a morphological change being observed for a discrete $[CO_3^{2-}]$ [10]. The supersaturation curve in Fig. 9 shows that increasing the carbonate ion concentration promotes the supersaturation of the carbonate (calcite and aragonite) phases such that gradually less ACP (and subsequently HA) is able to form. Carbonate ions may be incorporated into the ACP precursor phase, or may only be included in the HA crystallites when they nucleate. The first model may be explained by the presence of the flake like morphologies seen at some carbonate ion concentrations (Fig. 6). These may be ACP sheets that contained sufficiently high carbonate levels that transformation to HA was not possible.

The size of the cellular apatite structure decreased with increasing $[CO_3^{2-}]$, as seen in Figs 2–5. This behavior is indicative of either an increasing nucleation rate of HA within the ACP sheets, or a slower growth rate after nucleation. However, non-stoichiometric HA (i.e. carbonate substituted HA) provides good growth sites and if more defects are present, faster growth is expected. It appears likely therefore that there is a higher nucleation rate of HA within the ACP sheets in solutions with higher carbonate ion concentrations. This observation is further evidence that CO_3^{2-} ions are incorporated into the ACP precursor.

3.3. FT-IR

Peaks diagnostic of CO_3^{2-} occur in the range 1650–1300 cm^{-1}, and are diagnostic of ν_3 vibrations attributed to surface carbonate ions whose occupancy is dependent on competition between PO_4 and CO_3 species. An FT-IR spectrum for a sample prepared at atmospheric carbonate concentration is shown in Fig. 10. The spectrum shows peaks diagnostic of HA and carbonate substitutions. As observed previously by Rehman and Bonfield [11], HA exhibit three distinct peaks around 600 cm^{-1} (633, 602 and 566 cm^{-1}). One of these peaks, at 633 cm^{-1}, is attributable to the bending vibration of non-bridging hydroxyls. A vibration due to these non-bridging hydroxyl species is also seen at 3571 cm^{-1} (stretching). The presence of these hydroxyl sites suggests that any carbonate substitution occurs at the phosphate sites in the lattice, i.e. type ''b'' substitution

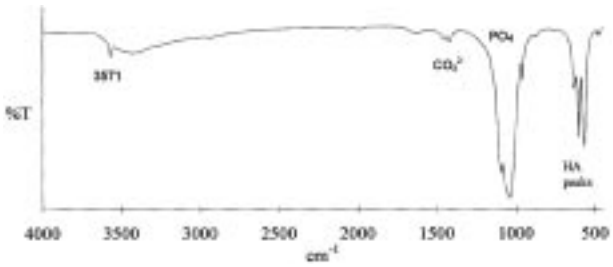

Figure 10 FT-IR spectrum for HA formed at atmospheric carbonate concentration.

4. Conclusions

A range of compositions from nearly stoichiometric HA through to pure calcium carbonate have been deposited in coating form. Included in the compositional range are coatings of carbonate substituted HA exhibiting a type ''b'' substitution, i.e CO_3^{2-} for OH^-. The size and morphology of the coating microstructure changed with increasing concentrations of carbonate ions. HA coatings are typified by a hexagonal, cellular microstructure. The decrease in cell size with increasing $[CO_3^{2-}]$ is attributed to an increased nucleation rate of HA within the ACP precursor gel. The pure calcium carbonate phases deposited have been identified as aragonite and calcite. These coatings were not as coherent as the HA coatings produced, and show no signs of the cellular microstructure which characterizes HA and carbonate substituted HA coatings. It is suggested that a phase which can act in an analogous way to the precursor ACP phase is required to produce a viable carbonate coating.

Acknowledgment

The authors would like to acknowledge Professor Brian Cantor for the provision of laboratory facilities. This work has been supported by The Wellcome Trust, under project numbers VS/96/OXF/014 and 048782.

References

1. K. DE GROOT, *J. Biomed. Mater. Res.* **21** (1987) 1375.
2. E. RUCKENSTEIN, S. GOURISANKER and R. BAYER, *J. Colloid. Interface. Sci.* **63** (1983) 245.
3. J. ONG and L. LUCAS, *Biomaterials.* **15** (1994) 337.
4. H. HERO, H. WIE, R. JORGENSEN and I. RUYTER, *J. Biomed. Mate. Res.* **28** (1994) 343.
5. R. LEGEROS, *Clin. Mater.* **14** (1993) 65.
6. T. KOKUBO, in ''Bone-Bonding Biomaterials'' (Reed Healthcare Communications, Netherlands, 1992) p. 102.
7. M. SHIRKANZADEH, M. AZADEGAN, V. STACK and S. SCHREYER, *Mater. Lett.* **18** (1994) 211.
8. S. BAN, J. HASEGAWA, S. MARUNO and T. HANAICHI, *Electro. Microsc.* **3B** (1994) 907.
9. A. PEAKER and J. CZERNUSZKA, *Thin Solid Films* **287** (1996) 174.
10. S. BERRY, in ''Biologically Active Coatings on Metallic Implants'' (Part II Thesis, Department of Materials, University of Oxford, UK, 1996).
11. I. REHMAN and W. BONFIELD, *J. Mater. Sci.: Mater. Med.* **8** (1997) 1.

Received 7 March
and accepted 3 August 1998